ROBotic Open-architecture Technology for
Cognition, Understanding and Behavior

Project No. 004370

RobotCub

Development of a Cognitive Humanoid Cub

Instrument: Integrated Project
Thematic Priority: IST - Cognitive Systems

D 5.1 Evaluation of an algorithm for interpreting the kinematics of arm motion and its relationship to object-directed motion

Due date: **01/03/2005 (+ 45 days)**
Submission Date: **15/04/2005**

Start date of project: **01/09/2004** Duration: **60 months**

Organisation name of lead contractor for this deliverable: **EPFL**

Responsible Person: **Prof. Aude Billard**

Revision: **1.0**

Project co-funded by the European Commission within the Sixth Framework Programme (2002-2006)		
Dissemination Level		
PU	Public	**PU**
PP	Restricted to other programme participants (including the Commission Service)	
RE	Restricted to a group specified by the consortium (including the Commission Service)	
CO	Confidential, only for members of the consortium (including the Commission Service)	

Contents

Abstract

We consider goal-directed reaching motions, in other words, reaching motions directed to an object of interest. This also includes pointing.
In this report, we present a model of human three-dimensional reaching movements. This model can quantatively and precisely match human reaching movement kinematics. The model is able to generate reaching and pointing movements, which are qualitatively similar to those of humans. It can also be used to predict ahead of time the target of a human reaching movement, by looking at the first part of the trajectory only.
Moreover, the model is consistent with a number of experimental findings on human reaching movement reported in the litterature.

1 Introduction

The aim of the work described in this document is to design a model for reaching motions intended to be implemented on a humanoid platform, allowing the robot to perform accurate reaching movements. Consistently with the developmental approach to robotics, this model should allow some degree of learning and adaptation and also serve as a building block to develop further cognitive abilities.
Furthermore, the modeling process should explore basic principles of movement control and multimodal fusion, that may be generalized to other cognitive tasks. More specifically, the idea of imitative communication and learning is kept in mind. To this end, the model should be multimodal and make a link between observed (possibly human) reaching movements and a corresponding (robot) motor action and proprioceptive feedback. This could allow a "motor perception" [11] on which imitative abilities could be developed. The model should thus at the same time allow for the synthesis and the analysis of reaching movements. In other words, it should allow the robot to generate reaching motions, but also to "understand" observed reaching motions. By "understanding" we here mean the ability to predict the target when observing the beginning of the movement only. This dual requirement of generation and prediction requires a trade-off between the generality required to account for the important variability of human reaching motions and the constraints needed for prediction.

The rest of this document is structured as follow. Section 2 reviews some important evidence and theoretical questions on human reaching motions. Section 3 describes an analysis of recorded reaching movements. Based on this analysis, a model of human reaching movements is presented in section 4. Based on this model, algorithms for reaching, pointing and movement prediction have been developed and tested on simulation. Of course, this model is far from comprehensive and constitute only a first, though encouraging, step. Directions for further development of the model are given in section 5. Section 6 concludes the document with some comments about the work accomplished so far. The mathematical technicalities and demonstrations figure in the appendix.

2 Human Reaching Movements

Traditionally, reaching has been (explicitly or implicitly) considered as a two-stage process. The first stage is the planning stage, which is followed by an execution stage [27]. According to this view, a reaching trajectory is computed during the planning stage, and the corresponding movement is actually performed during the execution stage. A large body of experiments and theories have been designed with this two-stage view of reaching movements in mind. They have thus investigated movement trajectory planning separately from the actual execution and control of the movement.

Investigations concerning movement planning sought mainly to determine the modality, or the frame of reference in which movements were planned. Some studies ([21],[1],[12]) suggested that movements were planned according to constraints expressed in a body-centered frame of reference, while others ([4] [17]) suggested that movements were planned according to intrinsic constraints expressed in joint angle coordinates. In all cases, invariant trajectory characteristics (in particular straight lines) in a given space were taken as evidence for that space being the planning space. After a careful review of the experimental settings of previous experiments, Desmurget *et al.*[8] showed that constraint settings where subjects were forced by a manipulandum to move in an horizontal plane induced straight spatial trajectories, whereas free settings induced straight joint angle trajectories. It thus seems that movement are not planned in a particular space, and that multiple frame of reference are being used, with their importance varying according to context and task.
Other studies suggested that human reaching movement were "optimal" in some sense. Movement planning would then be understood as finding the trajectory that minimizes a given cost functional. Various optimization criteria were suggested, such as the minimum jerk [12] [14], minimum torque change [22], minimum work [28] or minimum effort [18][2]. Those models are generally speaking hard to evaluate, and give similar predictions (see [10] for a critical review of optimality models of reaching).

According to the traditional view, the second stage of reaching movements is the execution stage. The main question concerning this stage is how the planned trajectory is actually executed, and what control mechanisms allow the observed reliability and adaptability of reaching movements. It has been shown that humans can adapt reaching trajectories to new environmental constraints on the arm biomechanics (manipulandum) and to new force fields [26], thus suggesting the existence of an "internal model of external perturbing forces" [13]. Several reports also indicate the existence of an internal "forward model" that can predict ahead of time the position of the limb during reaching movements [31] [3].

Several scholars have suggested that a clear-cut separation between a planning and an execution stage is not appropriate. According to this view, which follows the dynamical systems approach to cognition and action described by Kelso [16], there is no explicit trajectory planning, but rather an implicit set of trajectories specified by some attractor landscape. So there is no planned "preferred" trajectory that the system tries to match during execution, but a set of dynamic laws that move the system from one point to another, eventually leading it to the goal. The variables and nature of those dynamic laws remain to be fully determined, although some attempts have been made such as muscle stiffness and contraction in Bizzi's equilibrium point hypothesis [5], Lee's time-to-closure (tau)[19], or the stochastic optimal feedback control law suggested by Todorov and Jordan [30].
This approach to reaching movements offers an attractive explanation of the observed reliability and variability of human reaching movements. Only the variables relevant to goal achievement are controlled, leaving an "uncontrolled manifold" [25] of varying goal-irrelevant variables, while the relevant variables are inexorably attracted to the goal, in spite of possible perturbations.

With this in mind, we can conclude that any comprehensive model of reaching movements should account not only for the observed characteristics of reaching movement trajectories (quasi-straight paths, bell-shaped velocity profiles that scale with movement amplitude, speed-accuracy trade-off) but also for the intrinsic multimodality of those movements, and for their reliability [29]. Fitting such a model into the dynamical systems framework would probably be of great advantage.

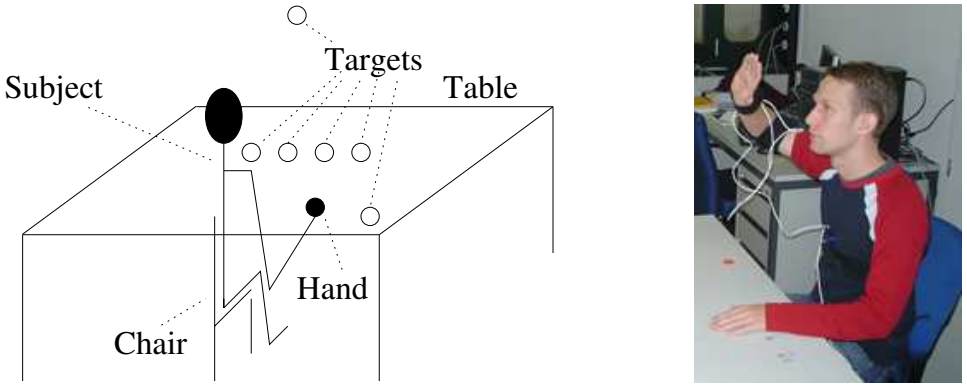

Figure 1: *Setup for reaching movement recording. On the left, a schematic drawing shows the locations of movement targets. There are 6 targets, five of which are on a table and one above the subject's head. The subject is represented in the starting position. On the right, a picture of a subject reaching above its head*

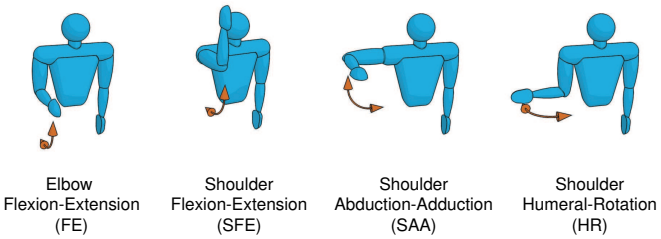

Figure 2: *The four degrees of freedom of the arm.*

3 Human Reaching Movement Analysis

3.1 Experimental Setup

Twenty different subjects were asked to perform unconstrained 3D reaching movements. Movement targets are shown as unfilled circles on Figure 1 (left). Five of six targets are on the table, while one target is above the subject's head. A total of 76 movements were recorded. The kinematics of the movements are measured using Xsens sensors and four joint angle trajectories (one for each joint of Figure 2) are extracted for each reaching movement. Those four joints (three at the shoulder and one at the elbow) capture the essential features of reaching movements. They can model the human arm and forearm movements (and not wrist movements). Cartesian endpoint trajectories can then be reconstructed using a direct geometrical model. The data was partitioned into a training set (48 movements) and a testing set (28 movements).

3.2 Analysis

Two kinds of data analysis were performed. The first analysis is a Principal Component Analysis (PCA) of the trajectories. PCA finds the trajectory components that best represent the data (in a mean square sense). The second analysis is an Independent Component Analysis (ICA). ICA finds

joint angle values		end point coordinates	
PCA	ICA	PCA	ICA
98.80	98.77	97.61	97.61

Table 1: *The results of the analysis. The percentage of variance of the testing set explained by the components of the training set.*

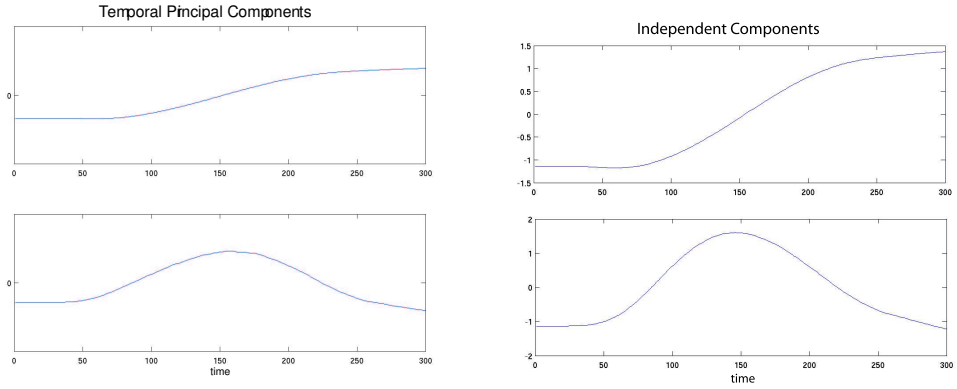

Figure 3: *The components for the joint angle trajectories. On the left figure, the two principal components obtained by PCA. On the right the two independent components obtained by ICA. The two methods yield similar components.*

the trajectory components which are most (statistically) independent from each other (see [15] for a detailed description of ICA).

3.3 Results

The training set was analyzed, and the two principal (or independent) components were derived. It was then computed how well those two components fitted the testing set. As an evaluation criterion, the percentage of explained variance was taken. This criterion is equivalent to a mean square fitting criterion. The results are displayed in Table 1 which shows the percentage of the testing set variance explained by the training set components. The analysis were performed on the joint angle trajectories as well as for the endpoint cartesian trajectories.
Those results indicate that PCA and ICA capture the major features of reaching movement data, since those features generalize to unseen data (more than 97% of variance explained). Moreover one can see that PCA and ICA are more or less equivalent in terms of performance.

Comparing the components returned by PCA and ICA (see Figure 3), one can notice that they are very similar. This similarity indicates that those components seem to maximize the variance of the data, as well as their independence. In the next section, a theoretical model builds on the characteristics of those components.

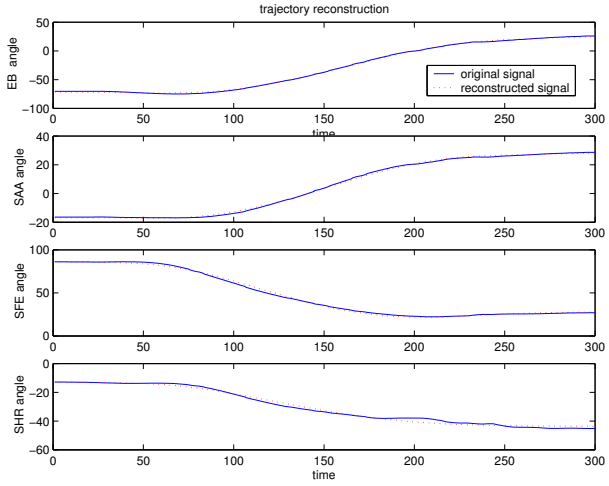

Figure 4: *Examples of reconstruction of the joint angle trajectories with two principal components. The solid lines represent the recorded raw data, the dotted line represent the approximation of this data using only two components.*

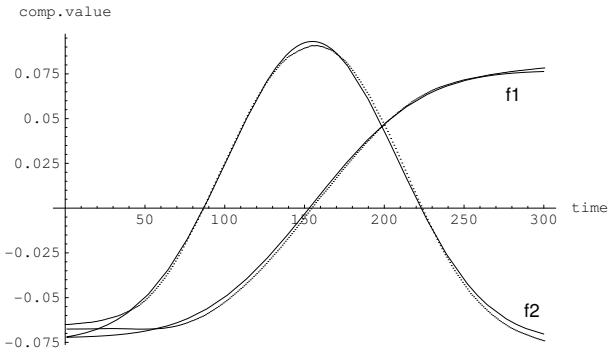

Figure 5: *The principal components (for the joint angle data) and their fitting functions*

4 A Model of Human Reaching Movements

4.1 Description

The previous section has shown that PCA and ICA yield a good representation of the reaching data, especially of joint angle trajectories. PCA and ICA with two components correspond to the following model.

$$\theta_i(t) = a_0^i + a_1^i f_1(t) + a_2^i f_2(t), \tag{1}$$

where $\theta_i(t), i = 1..4$ are the four joint angles trajectories (see Figure 2) , $f_1(t)$ and $f_2(t)$ are the principal (or independent) components.
As can be seen on Figure 3, the second component looks much like the derivative of the first component. The second component was approximated with a gaussian function, and the first component was approximated as the integral of the second component. This yields the following expression for

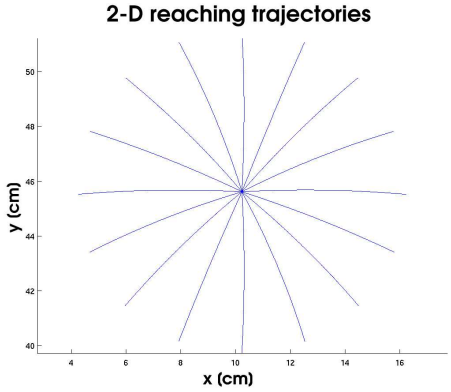

Figure 6: *Generated reaching motions in various directions. The motions are located in an horizontal plane, the bottom of the picture correspond to the direction to the body.*

components f_1 and f_2.

$$f_1(t) = \int_0^t c \cdot \exp\{\frac{(\tau - t_0)^2}{2\sigma^2}\} d\tau \quad (2)$$

$$f_2(t) = c \cdot \exp\{\frac{(t - t_0)^2}{2\sigma^2}\} = f_1'(t) \quad (3)$$

As can be seen on Figure 5, this model gives a good fit of the data. It captures 97.99% of the joint angle data variance and 96.79% of the cartesian data variance.

4.2 Reaching Movement Generation

Reaching a target point $\mathbf{x_T}$ in cartesian space is achieved by finding the parameter $\mathbf{A} = [\mathbf{a_0}\ \mathbf{a_1}\ \mathbf{a_2}]$ that produce the appropriate movement. This is done according to a gradient descent (in parameter space) of the squared distance of the hand to the target.

$$\Delta \mathbf{a_1} = -\mathrm{grad}_{\mathbf{a_1}}\left(\left(K(\theta(\mathbf{t_f})) - \mathbf{x_T}\right)^2 \right) \quad (4)$$

where $K(\theta)$ is the forward kinematic function and t_f end time of the movement. Matrix A is initialized such that $\mathbf{a_0} = \theta(\mathbf{0})$ and $\mathbf{a_1} = \mathbf{a_2} = 0$ (which corresponds to staying in the actual position).

In order to evaluate our reaching algorithm, we generated trajectories corresponding to the classical "center-out task", where a subject is asked to perform reaching motions in all directions on an horizontal plane. This task often appears in the literature on reaching movements (see for example [20]). The corresponding generated "center-out" trajectories are shown in Figure 6. The movement are qualitatively similar to human reaching movements.

4.3 Pointing

The dynamics of pointing motions is similar to that of reaching motions. It, however, entails an additional constraint on the direction $\mathbf{v}$ in which the wrist-hand vector points to. In our model, this

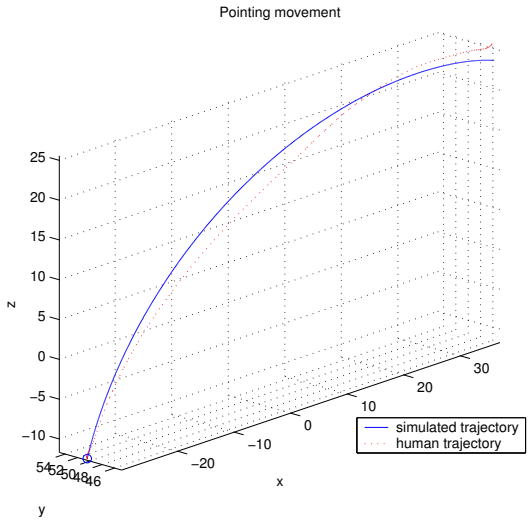

Figure 7: *A generated pointing movement. The dotted line corresponds to a recorded human pointing movement. The solid line correspond the the generated pointing movement when the pointing direction(*$\mathbf{v}$ *in equation 5) is set equal to that of the human. The trajectories are similar.*

constraint is applied by maximizing the dot product of the normalized movement speed vector and $\mathbf{v}$.

$$\begin{cases} \Delta \mathbf{a_1} &= -\text{grad}_{\mathbf{a_1}}\left(\left(\mathbf{K}(\theta(\mathbf{t_T})) - \mathbf{x_T}\right)^2 \right) \\ \Delta \mathbf{A} &= \text{grad}_{\mathbf{A}}\left(\frac{\mathbf{K}'(\theta(\mathbf{t_T}))^T}{\|\mathbf{K}'(\theta(\mathbf{t_T}))\|} \cdot \mathbf{v} \right) \end{cases} \tag{5}$$

In order to have a qualitative evaluation of our pointing algorithm, additional human reaching movements were recorded (using Xsens sensors). Taking the same initial arm posture and final hand location and movement direction a trajectory was generated using the algorithm described above. This trajectory was then compared to the human trajectory. An example is given in Figure 7.

4.4 Prediction

This model can be used to predict observed movements. By considering only the beginning of a movement, it is possible to find the parameters $\mathbf{A}$ of the model that best match this subpart of the motion. Those parameters can then be used to predict the following unseen part of the trajectory and, thus, the movement target (see appendix A.2 for the corresponding mathematical developments). An example is shown in Figure 8. One can see that after observing the first half of the movement and still about 35 cm away from the movement target, the model predicts the location of the target with a 7 cm error (stars). This error reduces to 3 cm after having seen three quarters of the movement (green square), and disappears almost completely by the end of the movement.
The example of Figure 8 shows a relatively favorable case, which can unfortunately not be generalized to all observed movements. This is due to the fact that only joint angle trajectories are taken into account for the prediction. In real settings, other cues and the cartesian trajectory can help the prediction. The prediction performance will be later compared to human prediction abilities in a similar setting (no external cue).

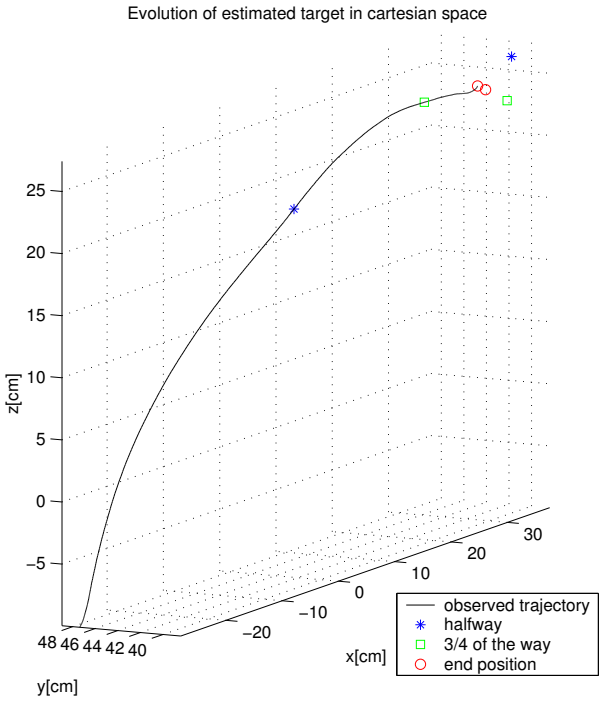

Figure 8: *Movement prediction. The solid line represent the hand path of the observed trajectory. After observing half of the movement (up to the star on the solid line - still some 40 cm away from target) the model prediction for trajectory end point (second blue star off the solid line) lies 7 cm away from the actual trajectory endpoint (circle). After observing three quarters (square - 20 cm away from target) of the trajectory, the endpoint prediction lies 3 cm away from the actual endpoint. The movement is the same as the one used to test the pointing (Figure 7)*

5 Discussion and Future Work

The model described above is consistent with several reaching movements characteristics reported in the literature. It produces bell-shaped velocity profile and straight joint angle trajectories in an unconstrained setting [4]. According to our model the final arm posture depends on the initial hand position [28] [7] and one can observe linear synergies between joint angles [9] if the second principal component is low. Moreover, the produced trajectory do not depend on movement speed [23]. The functional representation used in the model (i.e. the trajectory is represented as a whole, not as a succession of via points) can account for the forward model suggested in the literature [31].

In section 2 we mentioned that a good model of reaching movement should take the multimodality of reaching motions into account and would most probably benefit from fitting in a dynamical systems framework. However, the model described above appears to be a kinematic proprioceptive model. Although it can account for many characteristics of human reaching motions, its relationship to multimodality and dynamical systems seems somewhat shaky at first sight. Nonetheless, a deeper look into the model reveals possible connections.
First of all, the results of the human reaching movement analysis shown in section 3 suggest that the hand cartesian trajectory could be modeled by the same model than the joint angle trajectories. The coupling of the two models could be done using a forward and inverse kinematics function in a probabilistic framework. This would yield a multimodal model involving the visual and the proprioceptive modalities.

Furthermore, it can be shown (see appendix A.3) that our kinematic model (equation 1) is equivalent to a dynamical model specifying the joint angle acceleration variation (or jerk) as a function of joint angle speed and acceleration. This equivalence makes a link between the kinematic and the dynamic sides of the model. In other words it links the motor and the proprioceptive modalities. Moreover, the dynamical model may serve as a basis for a dynamical system which would have the reaching target as an attractor. This would allow very robust reaching abilities which could then be implemented on a robotic platform.

6 Conclusion

This reports describes a model of reaching movements, which is currently under development. Although very simple and not yet complete, this model is consistent with experimental data and can produce reaching and pointing movements similar to those of human subjects. It can also predict (albeit not in all cases) a trajectory by observing just its beginning.
This model also opens interesting perspectives for future developments, in particular for the interaction of different modalities and may be fitted into a dynamical systems framework.
It remains to be seen how easily this model can transfer from humans to robots. The interdependence between mechanics and control (hardware and software) is not completely understood, and the adequacy of the traditional distinction between hardware and software to more biologically inspired approaches is not clear. Indeed, it has been suggested in [6] that differences in human and macaque reaching motions may in part result from different morphologies.

A Mathematical Developments

A.1 Extrema Values

In order to be able to generate acceptable joint angle trajectories, i.e. trajectories that bounded in the range of reachable joint angle values, one has to know the extrema of the trajectories. The trajectories $\theta(t)$ are given by equations 1 to 3. The extrema are found by setting the derivative to zero:

$$0 = \dot{\theta}(t) = \frac{\partial}{dt}\big(a_0 + a_1 f_1(t) + a_2 f_2(t)\big) = a_1 \dot{f}_1(t) + a_2 \dot{f}_2(t)$$

Since $\dot{f}_1 = f_2$, we have

$$-\frac{a_1}{a_2} = \frac{\dot{f}_2}{f_2}$$

Integrating on both sides from t_0 to t yields

$$\big[-\frac{a_1}{a_2}\tau\big]_{\tau=t_0}^{t} = \big[\log f_2(\tau)\big]_{\tau=t_0}^{t} \Rightarrow -\frac{a_1}{a_2}(t-t_0) = -\frac{(t-t_0)^2}{2\sigma^2}$$

It follows from this that

$$t = 2\sigma^2 \frac{a_1}{a_2} + t_0 \tag{6}$$

is the time value for which $\theta(t)$ reaches its extrema.
From this formula, we derive the fact that there is only one extrema (apart from the extremities of the trajectory), which location depends only on the ratio $\frac{a_1}{a_2}$. Having a different ratio for two joints, induces a phase shift between those two joint angle trajectories.

A.2 Prediction

This section shows how to predict the movement trajectory having seen it only up to time τ.
For each joint angle we have an observation row vector $\theta^{\tau}_{\mathbf{obs}}$ of values for times ranging from 0 to τ. We want to find a_0, a_1 and a_2 such that

$$\big(\theta^{\tau}_{\mathbf{obs}} - (a_0 + a_1 \mathbf{f^{\tau}_1} + a_2 \mathbf{f^{\tau}_2})\big)^2, \tag{7}$$

(where the $\mathbf{f^{\tau}_i}$ are the components given by equation 2 and 3 up to time τ) is minimal. This can be achieved by projecting $\theta^{\tau}_{\mathbf{obs}}$ on the subspace spanned by $\mathbf{f^{\tau}_1}$, $\mathbf{f^{\tau}_2}$ and $\mathbf{f^{\tau}_0}$, a vector of same size containing only ones. In order to do the projection, one first has to find an orthonormal basis for this subspace. This is done using the Gram-Schmidt othonormalization procedure and the following orthonormal basis $\{f'_0,\ f'_1,\ f'_2\}$ is derived:

$$f'_0 = \frac{f^{\tau}_0}{\|f^{\tau}_0\|} \tag{8}$$

$$f'_1 = \frac{f^{\tau}_1 - < f'_0, f^{\tau}_1 > f'_0}{\|f^{\tau}_1 - < f'_0, f^{\tau}_1 > f'_0\|} \tag{9}$$

$$f'_2 = \frac{f^{\tau}_2 - < f'_0, f^{\tau}_2 > f'_0 - < f'_1, f^{\tau}_2 > f'_1}{\|f^{\tau}_2 - < f'_0, f^{\tau}_2 > f'_0 - < f'_1, f^{\tau}_2 > f'_1\|}, \tag{10}$$

where $<,>$ denotes the standard dot product: $< f, g >= \int f(t)g(t)dt$, and $\| \cdot \|$ is the corresponding norm ($\|f\| =< f, f >^{1/2}$). The projections p_i of the observation vector θ^τ_{obs} on the basis vectors f_i are then given by:

$$
\begin{aligned}
p_0 &= < \theta^\tau_{obs}, f'_0 > && (11)\\
p_1 &= < \theta^\tau_{obs}, f'_1 > && (12)\\
p_2 &= < \theta^\tau_{obs}, f'_2 > && (13)\\
& && (14)
\end{aligned}
$$

Let us give a name to the denominators of expressions 8 and followings in order to simplify the notations:

$$
\begin{aligned}
n_0 &= \|f^\tau_0\| && (15)\\
n_1 &= \|f^\tau_1 - < f'_0, f^\tau_1 > f'_0\| && (16)\\
n_2 &= \|f^\tau_2 - < f'_0, f^\tau_2 > f'_0 - < f'_1, f^\tau_2 > f'_1\| && (17)
\end{aligned}
$$

The closest approximation of the observation within the space defined by the basis is given by θ_p:

$$
\begin{aligned}
\theta^\tau_{obs} &\approx p_0 f'_0 + p_1 f'_1 + p_2 f'_2\\
&= p_0 \frac{f^\tau_0}{n_0} + p_1 \frac{f_1 - < f'_0, f^\tau_1 > f'_0}{n_1} + p_2 \frac{f^\tau_2 - < f'_0, f^\tau_2 > f'_0 - < f'_1, f^\tau_2 > f'_1}{n_2}\\
&= \frac{p_0}{n_0} f^\tau_0 + \frac{p_1}{n_1}\big(f^\tau_1 - \frac{< f'_0, f^\tau_1 >}{n_0} f^\tau_0\big) +\\
&\quad \frac{p_2}{n_2}\Big(f^\tau_2 - \frac{< f'_1, f^\tau_2 >}{n_1}\big(f^\tau_1 - \frac{< f'_0, f^\tau_1 >}{n_0} f^\tau_0\big) - \frac{< f'_0, f^\tau_2 >}{n_0} f^\tau_0\Big)\\
&= \hat{a}^\tau_0 f^\tau_0 + \hat{a}^\tau_1 f^\tau_1 + \hat{a}^\tau_2 f^\tau_2 && (18)
\end{aligned}
$$

Grouping the terms in the preceding equation yields the estimates $\hat{a}^\tau_0$, $\hat{a}^\tau_1$ and $\hat{a}^\tau_2$ of a_0, a_1 and a_2 respectively at time τ:

$$
\begin{aligned}
\hat{a}^\tau_0 &= \frac{1}{n_0}\Big(p_0 - \frac{p_1}{n_1} < f'_0, f^\tau_1 > + \frac{p_2}{n_2}\big(\frac{< f'_1, f^\tau_2 >< f'_0, f^\tau_1 >}{n_1} - < f'_0, f_2 >\big)\Big) && (19)\\
\hat{a}^\tau_1 &= \frac{1}{n_1}\big(p_1 - \frac{p_2}{n_2} < f'_1, f^\tau_2 >\big) && (20)\\
\hat{a}^\tau_2 &= \frac{p_2}{n_2} && (21)
\end{aligned}
$$

If one wants to weigh the observations according to a function $\omega(t)$, in order for example to give more importance to the recent observations and to forget old observations, one can use the same formulas but introduce the weighting factor into the dot product (i.e. $< f, g >= \int f(t)g(t)\omega(t)dt$).

A.3 Dynamical Model

This section follows the methodology described in section 13.4.2 of [24]. The aim of this section is to show the existence of and to derive a dynamical model corresponding to the kinematic model described by equations 1 to 3 . This model states that the trajectories are linear combination of the

following three functions:

$$f_0(t) = 1 \tag{22}$$

$$f_1(t) = \int_{t_s}^{t} \exp\{\frac{-\tau^2}{2}\} d\tau \tag{23}$$

$$f_2(t) = \exp\{\frac{(t^2}{2}\} = f_1'(t) \tag{24}$$

In order to simplify the computation, we have replace $t - t_0/\sigma$ by t, which corresponds to a shifting and scaling of the time. Those function can be gathered in a base vector $\mathbf{f(t)} = [f_0(t)\ f_1(t)\ f_2 t]^T$. Equation 1 can then be rewritten:

$$\theta(t) = \mathbf{a}^T \mathbf{f(t)}, \tag{25}$$

where $\mathbf{a} = [a_0\ a_1\ a_2]^T$, and where the indexes i have been dropped.
The dynamical model is defined by a vector of functions $\mathbf{w(t)} = [w_0(t)\ w_1(t)\ w_2(t)]^T$ such that:

$$\dddot{\theta}(t) = w_0(t)\theta(t) + w_1(t)\dot{\theta}(t) + w_2(t)\ddot{\theta}(t) \tag{26}$$

Expressing in a matrix form and inserting equation 25, one obtains:

$$\mathbf{a}^T \dddot{\mathbf{f}} = \mathbf{a}^T [\mathbf{f}\ \dot{\mathbf{f}}\ \ddot{\mathbf{f}}]\mathbf{w}, \tag{27}$$

where the argument t of the functions has been dropped. The matrix $[\mathbf{f}\ \dot{\mathbf{f}}\ \ddot{\mathbf{f}}] = \mathbf{W}$ is the third-order Wronskian matrix of the system defined by $\mathbf{f}$. Solving equation 27 with respect to $\mathbf{w}$ yields:

$$\mathbf{w} = \mathbf{W}^{-1} \dddot{\mathbf{f}} \tag{28}$$

For this to be an acceptable solution $\mathbf{W}$ must be invertible for any t. In order to check this, we first define:

$$f_3(t) = \dot{f}_2(t) = -t \exp\{-\frac{t^2}{2}\} = -t f_2(t) \tag{29}$$

$$f_4(t) = \ddot{f}_2(t) = (t^2 - 1) \exp\{-\frac{t^2}{2}\} = (t^2 - 1) f_2(t) \tag{30}$$

$$f_5(t) = \dddot{f}_2(t) = -t(t^2 - 3) \exp\{-\frac{t^2}{2}\} = -t(t^2 - 3) f_2(t). \tag{31}$$

Taking the derivatives of the basis functions, the Wronskian matrix is given by

$$\mathbf{W} = \begin{pmatrix} 1 & 0 & 0 \\ f_1 & f_2 & f_3 \\ f_2 & f_3 & f_4 \end{pmatrix}. \tag{32}$$

The determinant is then given by:

$$|\mathbf{W}| = f_2 f_4 - f_3^2 = (t^2 - 1 - t^2) f_2(t)^2 = -\exp\{-\frac{t^2}{2}\}^2 \tag{33}$$

Since this value is strictly negative for any t, the Wronskian matrix is invertible, and therefore there exists a dynamical model, which can be computed according to equation 28. Inverting the Wronskian

matrix yields

$$\begin{aligned}\mathbf{W}^{-1} &= \frac{1}{f_2^2}\begin{pmatrix} f_2^2 & 0 & 0 \\ f_1 f_4 - f_3 f_2 & -f_4 & f_3 \\ -f_3 f_1 + f_2^2 & f_3 & -f_2 \end{pmatrix} \\ &= \frac{1}{f_2(t)}\begin{pmatrix} f_2(t) & 0 & 0 \\ (t^2-1)f_1(t) - f_3(t) & -(t^2-1) & -t \\ t f_1(t) + f_2(t) & -t & -1 \end{pmatrix} \end{aligned} \tag{34}$$

Thus we have

$$\begin{aligned}\mathbf{w}(\mathbf{t}) &= \mathbf{W}(\mathbf{t})^{-1}\dddot{\mathbf{f}}(\mathbf{t}) = \mathbf{W}^{-1}\begin{pmatrix} 0 \\ f_4 \\ f_5 \end{pmatrix} \\ &= \begin{pmatrix} 0 \\ -(t^2-1)^2 - t^2(-t^2+3) \\ -t(t^2-1) + t(t^2-3) \end{pmatrix} = \begin{pmatrix} 0 \\ -(t^2+1) \\ -2t \end{pmatrix} \end{aligned} \tag{35}$$

The dynamical model can then be be expressed as

$$\dddot{\theta}(t) = -(t^2+1)\dot{\theta}(t) - 2t\ddot{\theta}(t) \tag{36}$$

.

References

[1] W. Abend, E. Bizzi, and P. Morasso. Human arm trajectory formation. *Brain*, 105:331–348, 1982.

[2] R. McN. Alexander. A minimum energy cost hypothesis for human arm trajectories. *Biological Cybernetics*, 76:97–105, 1997.

[3] G. Ariff, O. Donchin, T. Nanayakkaran, and R. Shadmehr. A real-time state predictor in motor control: Study of saccadic eye movements during unseen reaching movements. *The Journal of Neuroscience*, 22:7721–7729, September 2002.

[4] C.G. Atkeson and J.M. Hollerbach. Kinematic features of unrestrained vertical arm movements. *The Journal of Neuroscience*, 5(9):2318–2330, 1985.

[5] E. Bizzi, N. Accornero, W. Chapple, and N. Hogan. Posture control and trajectory formation during arm movement. *The Journal of Neuroscience*, 4:2738–2744, 1984.

[6] M.I. Christel and A. Billard. Comparison between macaques' and humans' kinematics of prehension: the role of morphological differences and control mechanisms. *Behavioural Brain Research*, 131:169–184, 2002.

[7] M. Desmurget, H. Gréa, and C. Prablanc. Final posture of the upper limb depends on the initial position of the hand during prehension movements. *Experimental Brain Research*, 119:411–516, 1998.

[8] M. Desmurget, M. Jordan, C. Prablanc, and M. Jeannerod. Constrained and unconstrained movements involve different control strategies. *Journal of Neurophysiology*, 77:1644–1650, 1997.

[9] M. Desmurget, C. Prablanc, Y. Rossetti, M. Arzi, Y. Paulignan, C. Urquizar, and J-C. Mignot. Postural and synergic control for three-dimensional movements of reaching and grasping. *Journal of Neurophysiology*, 74(2):905–910, 1995.

[10] S. Engelbrecht. Minimum principles in motor control. *Journal of Mathematical Psychology*, 45(3):497–452, 2001.

[11] L. Fadiga, L. Fogassi, V. Gallese, and G. Rizzolatti. Visuomotor neurons: ambiguity of the discharge or 'motor' perception? *International Journal of Psychophysiology*, 35:165–177, 2000.

[12] T. Flash and N. Hogan. The coordination of arm movements: An experimentally confirmed mathematical model. *The Journal of Neuroscience*, 5(7):1688–1703, 1985.

[13] F. Gandolfo, F.A. Mussa-Ivaldi, and E. Bizzi. Motor learning by field approximation. *Proceedings of the National Academy of Science USA*, 93:3843–3846, 1996.

[14] N. Hogan. An organizing principle for a class of voluntary arm movements. *Journal of Neuroscience*, 4(11):2745–2754, 1984.

[15] A. Hyvärinen, J. Karhunen, and E. Oja. *Independent Component Analysis*. John Wiley & Sons, Inc, 2001.

[16] J.A.S. Kelso. *Dynamic Patterns: The Self-Organization of Brain and Behaviour*. MIT Press, Cambridge, Massachusetts, 1995.

[17] F. Lacquaniti, J.F. Soechting, and S.A. Terzuolo. Path constraints on point-to-point arm movements in three-dimensional space. *Neuroscience*, 17(2):313–324, 1986.

[18] Ning Lan. Analysis of an optimal control model of multi-joint arm movements. *Biological Cybernetics*, 1997.

[19] D.N. Lee, C.M. Craig, and A. Grealy. Sensory and intrisic coordination of movement. *Proceedings of the Royal Society London B*, 266:2029–2035, 1999.

[20] J. Messier and J.F. Kalaska. Comparison of variability of initial kinematics and endpoints of reaching movements. *Experimental Brain Research*, 125:139–152, 1999.

[21] P. Morasso. Spatial control of arm movements. *Experimental Brain Research*, 42:223–227, 1981.

[22] E. Nakano, H. Imamizu, Y. Uno, H. Gomi, T Yoshioka, and M. Kawato. Quantitative examinations of internal representations for arm trajectory planning: Minimum commanded torque change model. *Journal of Neurophysiology*, 81:2140–2155, 1999.

[23] K.C. Nishikawa, S.T. Murray, and M. Flanders. Do arm postures vary with the speed of reaching? *Journal of Neurophysiology*, 81:2582–2586, 1999.

[24] J.O. Ramsay and B.W. Silverman. *Functional Data Analysis*. Springer, 1997.

[25] J.P. Scholz and G. Schöner. The uncontrolled manifold concept: identifying control variables for a functional task. *Experimental Brain Research*, 126:289–306, 1999.

[26] R. Shadmehr and F.A. Mussa-Ivaldi. Adaptive representation of dynamics during learning of a motor task. *The Journal of Neuroscience*, 14:3208–3224, May 1994.

[27] R. Shadmehr and S.P. Wise. *The Computational Neurobiology of Reaching and Pointing*. The MIT Press, 2005.

[28] J.F. Soechting, C.A Buneo, and M. Flanders. Moving effortlessly in three dimensions: Does Donder's law apply to arm movement? *Journal of Neuroscience*, 15(9):6271–6280, 1995.

[29] E. Todorov. *Studies of Goal Directed Movements*. PhD thesis, Massachussetts Institute of Technology, 1998.

[30] E. Todorov and M.I. Jordan. Optimal feedback control as a theory of motor coordination. *Nature Neuroscience*, 5(11):1226–1235, 2002.

[31] D. Wolpert, Z. Ghahramani, and M.I. Jordan. An internal model for sensorimotor integration. *Science*, 269(5232):1880–1882, 1995.